Diffusion Limited Crystallization and Phase Partitioning in ZrO$_2$-Metal Oxide Binary Systems

Code: D3

F.F. LANGE, M.L. BALMER AND C.G. LEVI

Materials Department, College of Engineering, University of California at Santa Barbara, Santa Barbara, CA 93106

Abstract. Chemical routes to synthesize inorganics can start with solutions where multiple elements remain well mixed during liquid evaporation, precursor decomposition and crystallization. Because crystallization generally occurs at temperatures where diffusion is very limited, a single phase can crystallize with a greatly extended solid-solution that does not achieve its equilibrium phase assemblage until much higher temperatures where diffusion is no longer constrained. Partitioning at these higher temperatures can lead to unique microstructures such as the nano-composite illustrated here for a metastable $Zr_{(1-x)}Al_xO_{2-x/2}$ ($x \leq 0.57$) phase that partitions into a composite containing t-ZrO$_2$ grains and α-Al$_2$O$_3$ plates.

Keywords: diffusion-limited crystallization, phase diagrams, metastability, ZrO$_2$-metal oxide

1. Introduction

Chemical processing routes which initiate with a solution are often used to produce ceramic powders, fibers and thin films. A variety of solution chemistries exist for multi-element compositions that yield solid-like gel precursors which are resistant to partitioning prior to decomposition into the desired inorganic compound. Because the decomposition temperature is very low, the driving potential for crystallization is very large. In addition, the critical nucleation size required for spontaneous crystallization is very small. Because the free energy of crystallization is high and the critical nucleation size is small, inorganic materials synthesized from precursors crystallize to nano-meter, polycrystalline microstructure at low homologous temperatures. At low crystallization temperatures, long range diffusion is inhibited and partitioning to equilibrium phase assemblages is kinetically constrained. Crystallization under conditions of kinetically limited diffusion conditions allows the synthesis of phases with various forms of metastability, including extended solubility, non-equilibrium structures, disorder in ordered structures, etc. In addition, novel microstructures, e.g., nano-

composites can be produced when a single, metastable phase partitions to its equilibrium phase assemblage.

The understanding of diffusion-limited crystallization can be used to predict the compositional phase fields for different metastable $Zr_{(1-x)}M_x^{+a}O_{2-x(4-a)/2}$ phases in the ZrO$_2$-Y$_2$O$_3$, –Gd$_2$O$_3$, –MgO and –Al$_2$O$_3$ binary systems [1–4]. As reviewed below, it has also been shown that the single metastable phase produced during low temperature crystallization can partition into either equilibrium phases [1] or other metastable phases prior to reaching the equilibrium phase assemblage [2, 3] at temperatures where the diffusional constraint is relieved. We also review how nano-composites are produced where two interpenetrating phases partition at high temperatures [2, 4].

2. Diffusion Limited Crystallization

The concept of diffusion limited crystallization will be illustrated with the ZrO$_2$–Al$_2$O$_3$ and ZrO$_2$–Gd$_2$O$_3$ binary systems. Pure zirconia has three polymorphic, fluorite based, structures: cubic → 2370°C → tetragonal → 1100°C → monoclinic. At equilibrium, Mg^{+2}, Ca^{+2}, Y^{+3}, trivalent rare-earth cations,
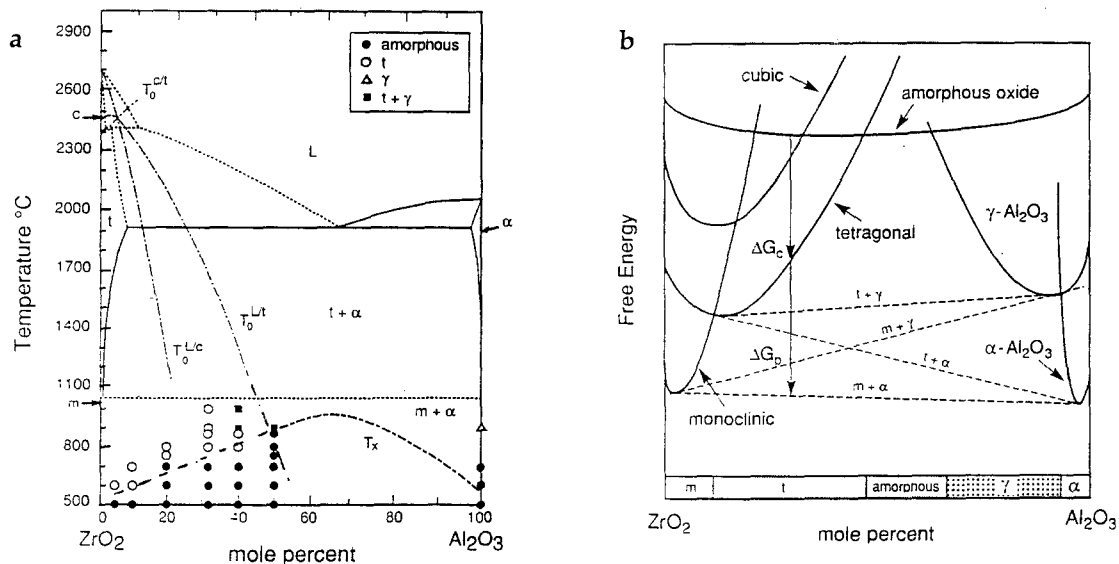
Fig. 1. a) Phase diagram for the ZrO_2–Al_2O_3 binary system. b) Free energy functions different structures of ZrO_2 and Al_2O_3 under conditions of diffusion limited crystallization.

Ce^{+4}, Ti^{+4}, etc. form extensive solid-solutions with ZrO_2 and dramatically alter the transformation temperatures. Aluminum oxide has one equilibrium structure, α-Al_2O_3 (corundum); it also has a number of metastable spinel-based structures which form readily when Al_2O_3 crystallizes from precursors [5] or during melt quenching [6–8]. The size of the octahedral or tetrahedral sites in the α-Al_2O_3 structure are unfavorable for extensive Zr^{+4} occupancy, which severely limits the equilibrium Al_2O_3 solubility in ZrO_2 to ≤ 2 mole % at temperatures $\leq 1400°C$ as shown by the phase diagram (Fig. 1a) determined by Alper and Stewart [9] and modified by Jayaram et al. [6]. The dashed line, represented by T_x, reports the crystallization temperature vs composition for rapid solidification experiments [6] (open and filled circles) and for compositions synthesized with two different solution precursors (alkoxide derived [10] and acetate/nitrate [4] derived) for $Zr_{(1-x)}Al_xO_{2-x/2}$ compositions ($x \leq 0.6$).

The broken lines represented by T_o are the temperature-compositional curves where two phases with identical compositions (e.g., L/t = Liquid + t–$(Zr, Al)O_2$) have the same free energy. Although T_o curves can be approximated with knowledge of the equilibrium diagram, they are generally determined through experiments where metastable phases are produced via either rapid solidification or precursor synthesis. T_o curves define metastable phase fields, e.g., all compositions to the left of the $T_o^{L/t}$ curve drawn on
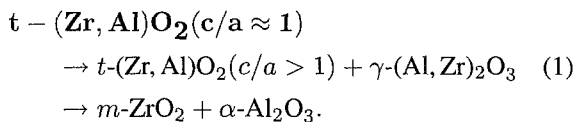
the equilibrium diagram in Fig. 1a are expected to crystallize with the tetragonal structure with an extended, metastable solid-solution composition. The T_o function is better illustrated in the ZrO_2 rich side of the ZrO_2–Gd_2O_3 binary as the curve that nearly divides the two phase, tetragonal + cubic, field.

Crystallization via either rapid cooling [6] or heating after precursor pyrolysis [4, 10] produces a single phase as schematically illustrated with the free energy vs composition diagram in Fig. 1b for temperatures within the range of crystallization (500°C to 900°C). The free energy functions for the m-, t- and c-ZrO_2, γ-, and α-Al_2O_3 structures are schematically plotted with experimental observations [4] [Intersections for different free energy functions define the T_o composition between the respective phases]. Figure 1b also shows the schematic free energy function for the amorphous (or liquid) phase.

Although Fig. 1b indicates that m-ZrO_2 and α-Al_2O_3 are the equilibrium phases within this temperature range, neither are observed during diffusion limited crystallization. Instead, for compositions containing ≤ 40 mole % Al_2O_3, the crystallization temperature is sufficiently low to kinetically constrain long-range diffusion during crystallization and only the tetragonal structure, with a greatly extended solid-solution, crystallizes [4]. Alumina rich compositions crystallize with the γ-Al_2O_3 structure with a large range of compositional solid-solubility. Compositions near the

center of the binary crystallize at higher temperatures where diffusion is not kinetically constrained, and thus concurrently crystallize and partition to produce two metastable phases, $viz.$, t-ZrO_2 and γ-Al_2O_3, both with greatly extended solid-solubility. Thus at temperatures where structural units within the amorphous phase have sufficient mobility to 'snap' into place to allow a critical nucleus to spontaneously grow, the composition crystallizes as a single phase without partitioning with a free energy reduction, per unit volume of ΔG_c. As the composition 'moves away' from the lowest free energy composition, the size of the critical nucleus for crystallization increases because ΔG_c decreases. Crystallization is thus delayed to higher temperatures where some long-range diffusion is required to form larger nuclei. When the composition is sufficiently different from the equilibrium compositions, the crystallization temperature can be too high to limit diffusion and prevent concurrent crystallization and phase partitioning. On the Al_2O_3 side of this binary, γ-Al_2O_3 is always observed during crystallization, apparently because the free energy difference between the α and γ structures is small.

When compositions that produce single, metastable structures during crystallization, are heated to temperatures where long-range diffusion is no longer kinetically limited, diffusion occurs, driven by partitioning free energy, ΔG_p, in an attempt to produce the equilibrium phase assemblage (m-ZrO_2 and α-Al_2O_3 for the temperature range considered). Because diffusion results in compositional gradients, a series of metastable phases with ranges of solid-solution can be observed prior to observing the equilibrium phases. For the ZrO_2-Al_2O_3 system, the observed partitioning sequence is [4]

$$t - (Zr, Al)O_2(c/a \approx 1)$$
$$\rightarrow t\text{-}(Zr, Al)O_2(c/a > 1) + \gamma\text{-}(Al, Zr)_2O_3 \quad (1)$$
$$\rightarrow m\text{-}ZrO_2 + \alpha\text{-}Al_2O_3.$$

Although the understanding of diffusion limited crystallization was initially developed for rapidly quenched metal alloys, it is obvious that diffusion limited crystallization also applies to the low temperature synthesis of materials from chemical precursors which initiate with well mixed solutions. Unlike rapid solidification, where the production of a metastable phase requires rapid heat exchange, diffusion limited crystallization *occurs during heating*. It is a natural phenomena for chemically derived materials.

3. Metastable Phases and Partitioning in the ZrO_2-RE_2O_3 Systems

Binary rare-earth (RE)-zirconia compositions fabricated by densifying powders, derived from precursor synthesized compositions, are dense, polycrystalline materials that exhibit high fracture toughness and strength due to a phenomena known as transformation toughening [1, 2]. The tetragonal grains in these materials, which undergo a stress-induced tetragonal to monoclinic transformation in front of a propagating crack, are the toughening agent. It is now known that the t-ZrO_2 in these materials is metastable phase because the powders are produced from chemical precursors that crystallize as the tetragonal structure with a greatly extended solid-solubility of the rare earth ion, and phase partitioning at the ceramic processing temperature is extremely sluggish [1]. Both the retention of the tetragonal toughening agent and its susceptibility to stress-induced transformation depends on the degree of partitioning [1] and thus the processing conditions (time and temperature).

The $T_o^{t/c}$ function, shown in Fig. 2a for the ZrO_2-Gd_2O_3 binary [2] is useful to predict what single, metastable phase is expect to crystallize during diffusion limited crystallization. At crystallization temperature for the Zr-acetate/Gd-nitrate precursors used to synthesize these materials ($\approx 450°C$), a metastable tetragonal phase crystallizes when the Gd_2O_3 content is < 6.5 moles % Gd_2O_3 (all compositions to the left of the $T_o^{t/c}$ curve), and a metastable cubic phase crystallizes when the Gd_2O_3 content is greater (right side of the $T_o^{t/c}$ curve).

At 1400°C, the maximum equilibrium solid-solubility of Gd_2O_3 in tetragonal ZrO_2 is 1.0 ± 0.1 mol% and the minimum equilibrium solid-solubility in cubic ZrO_2 is 8.0 ± 0.2 mol%. As shown in Fig. 2b complete partitioning of a metastable tetragonal phase containing 3 moles % Gd_2O_3 requires > 200 hr at 1400°C. Large compositional variations (± 1 mol% Gd_2O_3) were observed within tetragonal grains and from grain to grain during the first 50 h at 1400°C, whereas the composition of cubic grains produced during partitioning were relatively invariant. Experiments showed that this compositional variability was not present in material rapidly heated to 800°C, but was a result of partitioning.
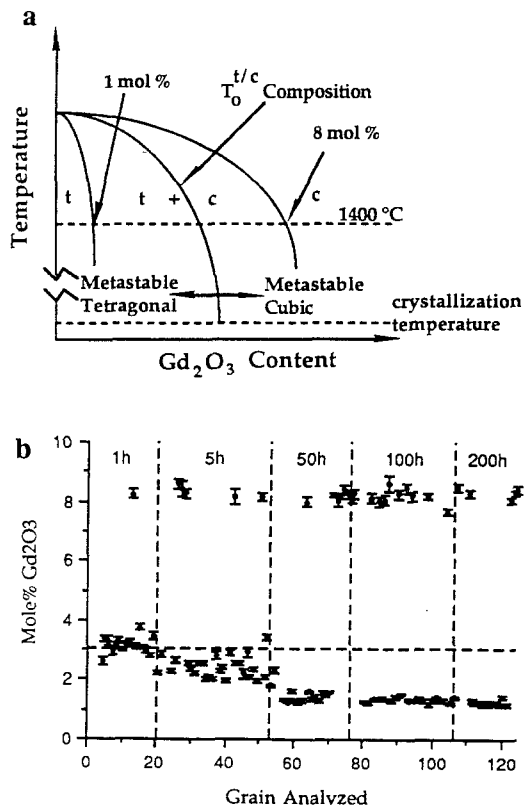
Fig. 2. a) Schematic of ZrO_2-rich end of the ZrO_2–Gd_2O_3 binary phase diagram showing the two-phase (t = tetragonal, c = cubic) field and the $T_o^{t/c}$ function. b) Grain by grain EDS analysis of Gd_2O_3 content vs heat treatment time at 1400°C for a composition containing 3 moles % Gd_2O_3 crystallized at 450°C from a Zr-acetate/Gd-nitrate precursor.

4. Phase Partitioning Produces Nano-Composites

When the volume fraction of the second phase is < 0.1 it can be considered an inclusion phase that can hinder grain growth as initially described by Zener, i.e., the inclusions hinder the motion of grain boundaries. Grain boundary motion only requires the short-range diffusion of the major phase; *viz.*, the cooperative hopping of atoms from one side of the grain boundary to the other. When the volume fraction of the second phase is greater than the percolation threshold (> 0.16), both the major and minor phases are percolating, and the microstructure consists of two interpenetrating phases. Under these conditions, Zener's concept is no longer valid, and the growth of either phase requires that both undergo long-range diffusion. Because long-range diffusion now controls the growth of either phase, interpen-
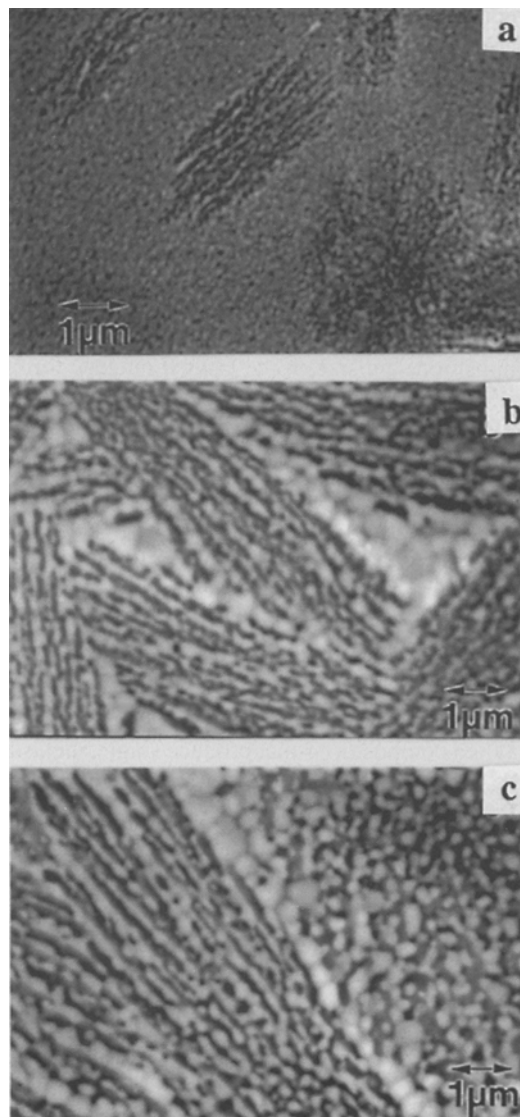
Fig. 3. Backscattered electron images of partitioned $Zr_{(1-x)}Al_xO_{(2-x/2)}$ containing the equivalent of 40 mol% Al_2O_3 (x = 0.57) heat treated at (a) 1200°C/1 h, (b) 1300°C/1 h and (c) 1400°C/1 h. at 1200°C α-Al_2O_3-rich regions grow as stacked plates within t-ZrO_2 + γ-Al_2O_3 two phase matrix.

etrating microstructures can be very stable at high temperatures.

As discussed above, the grain size of the polycrystalline, metastable, single phase produced during kinetic limited crystallization can be in the range of 20 to 50 mm during phase partitioning. Although the exact nature of the partitioning phenomenon is still uncertain (precipitation vs. spinodal) the size of the second phase grains (or precipitates) produced during

partitioning is comparable to the initial grain size of the metastable phase. When the volume fraction of the second phase exceeds that required for percolation (> 0.16), composite microstructures will be produced that will be relatively stable to grain growth at high temperatures. Since the grain size of both phases produced during partitioning are described in nano-meters, nano-composites, resistant to grain growth at high temperatures are produced.

The relatively stable, fine grain (≤ 300 nm) sized ZrO_2 materials produced in different ZrO_2-rare earth binary systems are due to the two interpenetrating phase microstructure produced as the initial metastable tetragonal phase partitions during processing at high temperatures [1, 2]. An example of another unique, nano-composite produced during phase partitioning is shown in Fig. 3. It was produced [4] by first partitioning a metastable $Zr_{(1-x)}Al_xO_{2-x/2}$ ($x = 0.57$) into a t-ZrO_2 + α-Al_2O_3 at temperatures $< 1200°C$, where grains of both phases are 50 to 100 nm in size. The γ-$Al_2O_3 \rightarrow \alpha$-$Al_2O_3$ transformation within this two phase material initiates at $\approx 1200°C$ [11]. As shown, the α-Al_2O_3 grains grow as stacked plates. All plates within a given 'stack' have a common nucleus, and thus, a common crystallographic orientation. Because the two phases (t-$ZrO_2 + \alpha$-Al_2O_3) are interpenetrating, and α-Al_2O_3 exhibits relatively little diffusion at $1400°C$, the microstructure shown in Fig. 3c remains invariant for at least 100 hr at $1400°C$ [11].

5. Concluding Remarks

The synthesis of metastable phases with greatly extended solid-solutions is a natural phenomena for materials synthesized from precursors where elements are well mixed in the solution state. The concept of diffusion limited crystallization explains why these metastable phases form, and can be used to detail the sequence of other metastable phases that form during partitioning at higher temperatures where diffusion is no longer constrained. Because the metastable phase crystallizes as nano-meter crystallites and partitioned phases are of the same dimension, stable nano-composites can be formed via this processing route.

Acknowledgment

References

1. Lange, F.F., Marshall, D.B., and Porter, J.R., "Controlling Microstructures Through Phase Partitioning From Metastable Precursors: The ZrO_2-Y_2O_3 System," p. 519–32 in *Ultra-structure Processing of Advanced Ceramics*. Edited by J.D. Mackenzie and D.R. Ulrich, John Wiley and Son, N.Y. (1988).

2. Leung, D.K., Chan, C.J., Ruhle, M., and Lange, F.F., "Metastable Crystallization, Phase Partitioning, and Grain Growth of ZrO_2–Gd_2O_3 Materials Processed from Liquid Precursors," J. Am. Ceram. Soc., 74 [11] 2786–92 (1991).

3. Balmer, M.L., Lange, F.F., and Levi, C.G., "Metastable Phase Selection and Partitioning in ZrO_2–MgO Processed from Liquid Precursors," J. Am. Cer. Soc., 75 [4] 946–52 (1992).

4. Mari Lou Balmer, Lange, Fred F., and Levi, Carlos, G., "Phase Selection and Extended Solubility in ZrO_2–Al_2O_3 Processed from Liquid Precursors," to be published.

5. Wilson, S.J. and McConnell, J.D.C., "A Kinetic Study of the System γ-AlOOH/Al_2O_3," J. Solid State Chem., 34, 315–22 (1980).

6. Jayaram, V., Levi, C.G., and Mehrabian, R., "Characterization of Al_2O_3–ZrO_2 Powders Produced by Electrohydrodynamic Atomization," Materials Science and Engineering, A124, 65–81 (1990).

7. Kalonji, G., McKittrick, J., and Hobbs, L.W., "Applications of Rapid Solidification Theory and Practice to Al_2O_3–ZrO_2 Ceramics,"; pp. 816–825 in Advances in Ceramics, Vol. 12, *Science and Technology of Zirconia II*, Edited by N. Claussen, M. Ruhle, and A.H., Heuer., American Ceramic Society, Columbus, OH, 1981.

8. Ando T. and Shiohara, Y., "Metastable Alumina Structures in Melt Extracted Alumina-25 wt% Zirconia and Alumina-42 wt% Zirconia Ceramics," J. Am. Cer. Soc., 74[2] 410–17 (1991).

9. Alper, A.M. and Stewart, G.H., (ed.), *Science of Ceramics*, Vol. 3, Academic Press, London, 1967, p. 339.

10. Yamaguchi, O., Shirai, M., and Yoshinaka, M., "Formation and Transformation of Cubiz ZrO_2 Solid Solutions in the System ZrO_2–Al_2O_3," J. Am. Cer. Soc., 71[12] C-510-C- 512 (1988).

11. Balmer, Mari, Lou, Lange Fred F. and Levi, Carlos, G. "Development of Nano-Composite Microstructures in ZrO_2–Al_2O_3 Via the Solution Precursor Method" Submitted to The Journal of the American Ceramic Society.